

Special Section:

Recent Progresses in Oceanography and Air-Sea Interactions in Southeast Asian Archipelago

Key Points:

- The Makassar Strait surface layer transport is affected by the Madden-Julian Oscillation during the boreal winter
- The MJO active phase may reduce the southward surface layer transport by up to 4 Sv
- Northward pressure gradient offsets the vertical divergence of Reynold stresses to force the northward transport during the MJO

Correspondence to:

A. M. Napitu,
asminapitu@caa.columbia.edu

Citation:

Napitu, A. M., Pujiana, K., & Gordon, A. L. (2019). The Madden-Julian Oscillation's impact on the Makassar Strait surface layer transport. *Journal of Geophysical Research: Oceans*, 124, 3538–3550. <https://doi.org/10.1029/2018JC014729>




Received 1 NOV 2018

Accepted 14 APR 2019

Accepted article online 30 APR 2019

Published online 5 JUN 2019

The Madden-Julian Oscillation's Impact on the Makassar Strait Surface Layer Transport

Asmi M. Napitu^{1,2} , Kandaga Pujiana^{3,4} , and Arnold L. Gordon¹ 

¹Lamont-Doherty Earth Observatory, Columbia University, Palisades, NY, USA, ²Institute for Marine Research and Observation, Ministry of Marine Affairs and Fisheries, Jakarta, Indonesia, ³Pacific Marine Environmental Laboratory, NOAA, Seattle, WA, USA, ⁴Faculty of Earth Sciences and Technology, Bandung Institute of Technology, Bandung, Indonesia

Abstract The Indonesian Throughflow (ITF) surface layer dynamics within the Makassar Strait, responsible for ~77% of the ITF, are investigated using in situ and satellite-derived observations from January 2004 to August 2011 and August 2013 to December 2016. Surface layer southward transport attains its minima during boreal winter in response to atmospheric and oceanic processes attributed to Australian-Indonesian monsoon as well as the Madden-Julian Oscillation (MJO). While the monsoon's impact on seasonal variability of the ITF transport has been well documented, the MJO's role to modulate the variability of the ITF transport is less studied. Eleven MJO events traversed from Indian Ocean to Western Pacific during boreal winter months over the course of the Makassar Strait time series. Intensified along-strait wind stress, reduced outgoing longwave radiation, increased sea surface height in the southern Makassar Strait, and a reduction in the surface layer ITF transport by up to 4 Sv marked the impact of the active phase of the MJO. Analysis of the momentum budget in the surface layer indicates that the excess of northward momentum due to the along-channel pressure gradient over northward momentum attributed to the vertical divergence of Reynold stress governs the northward acceleration of the surface layer during the MJO active phase.

1. Introduction

The Indonesian Throughflow (ITF), the flow of the Pacific water into the Indian Ocean via the Indonesian seas, governs the exchange of heat and freshwater fluxes between these two basins (Gordon, 1986; Sprintall et al., 2014). Observations in the Indonesian seas reveal that ITF variation spans a broad spectrum, encompassing timescales from intraseasonal to interannual (Gordon et al., 2010, 2012; Sprintall & Revelard, 2014). Discerning the underlying mechanisms governing the ITF variability is fundamental to obtain a better understanding of the ITF and its relationship to the larger-scale ocean and climate system.

The ITF demonstrates significant intraseasonal variability (20–90 days). ITF measurements in the Indonesian straits indicate that coastally trapped Kelvin waves with the Indian Ocean origin perturb ITF variability every 2–3 months beneath the pycnocline of Lombok, Ombai, and Makassar Straits (Figure 1; Drushka et al., 2010; Pujiana et al., 2013, 2009; Schiller et al., 2010). Planetary waves originating from the Pacific warm pool and locally generated shear instability account for the 1–2 months ITF variability observed in Makassar Strait (Chen et al., 2018; Pujiana et al., 2012).

Influences of Madden-Julian Oscillation (MJO), a prominent source of intraseasonal variability in the tropical atmosphere (Yoneyama et al., 2013; Zhang, 2013), on the ITF have been reported in previous studies. Zhou and Murtugudde (2010) and Shinoda et al. (2016) posited that westerly wind bursts attributed to the MJO across the equatorial Indian Ocean initiate the formation of Kelvin waves along the southern coast of Indonesian islands that penetrate into the ITF passages within the Indonesian seas, inducing ITF variability particularly at depths beneath the pycnocline. Response of surface layer ITF to the MJO remains an outstanding question.

Wind fields and ocean currents attributed to the Australian-Indonesian monsoon affect seasonal variation of the ITF transport (Potemra & Lukas, 1999; Sprintall et al., 2014). During the northwest monsoon months of December–March (henceforth referred to DJFM), northwesterly wind drives relatively buoyant South China

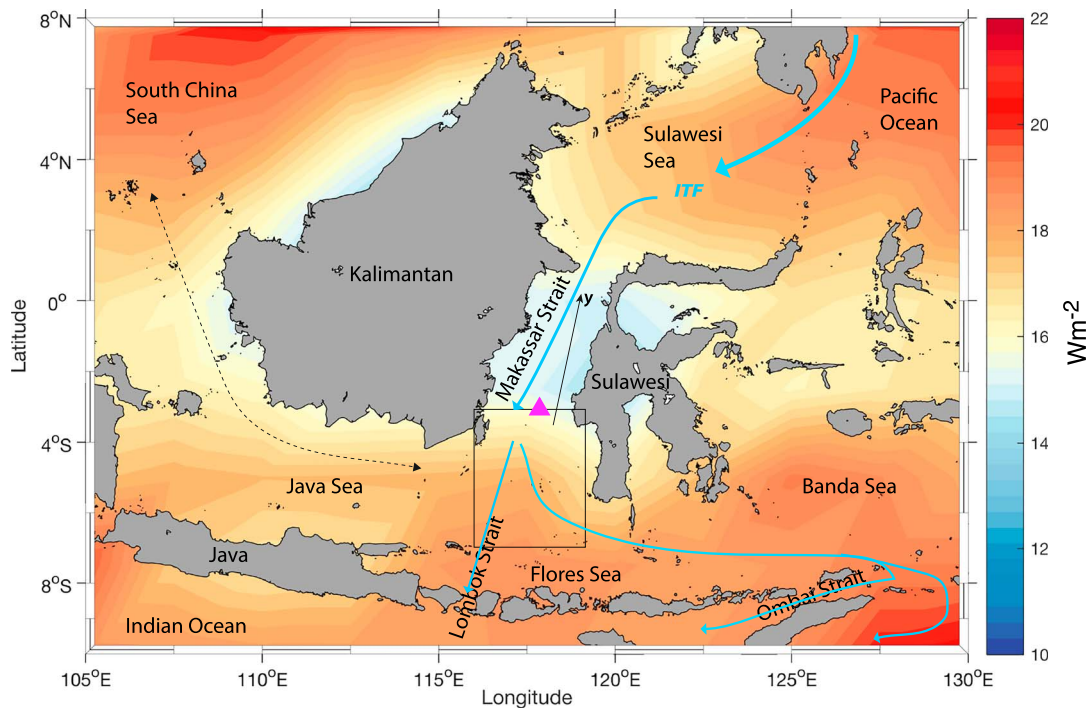


Figure 1. Standard deviations of outgoing longwave radiation (OLR) variability with timescales of 20–90 days, based on satellite-retrieved OLR data observed during 2004–2016 over the central Indonesian maritime continent. OLR data over land are masked. Triangle indicates mooring location in Makassar Strait. Solid arrows denote simplified pathway of the Indonesian Throughflow. Dashed arrow indicates simplified direction of South China Sea throughflow. The along strait axis in Makassar Strait (y) makes an angle of 10° relative to the true north. Black rectangle indicates the area where averages of OLR and zonal wind stress, τ^x , are computed.

Sea (SCS) surface layer water into the Indonesia seas (Figure 2b, left panel), which reduces the regional pressure head into the Indian Ocean and subsequently acts to retard the ITF transport within the upper 100 m of the water column (left panel of Figure 2a; Gordon et al., 2012).

In contrast, the opposite southeasterly winds prevailing over the course of the southeast monsoon through the months of June–September (henceforth referred to JJAS) remove the buoyant SCS water from the southern Makassar Strait (Figure 2, right panel), allowing the ITF to reach its maximum transport (Gordon et al., 2010, 2012, 2019). Thus, the upper layer ITF generally attains its minimum (maximum) transport through DJFM (JJAS). This seasonal variation of the ITF is sensitive to long-term, background conditions of regional climate such as El Niño–Southern Oscillation (ENSO). Under an El Niño condition, more buoyant SCS water is flushed into the Indonesian seas, strengthening the buoyant plug that further weakens the ITF (Gordon et al., 2012; Tozuka et al., 2007, 2009).

Despite ubiquitous intraseasonal variations in the lower troposphere of the tropics, for example, MJO, their impact on seasonal variability of near-surface ITF has not yet been investigated. Using ITF measurements in Makassar Strait spanning between 2004 and 2006, Pujiana et al. (2009) reported notable intraseasonal ITF variability in the upper layer during DJFM. Schiller et al. (2010), employing numerical experiments, arrived at a similar conclusion. The genesis accounting for the pronounced upper layer ITF variation at intraseasonal timescale during boreal winter has remained unexplained.

Through analyses of direct ITF measurements during 2004 to mid-2017 in Makassar Strait, we attempt to explore a direct link between the MJO and surface layer transport, which is substantial during the boreal winter (DJFM). The paper is organized as follows. Specifications of data and methods used in this study are given in section 2. Seasonal and intraseasonal variations of ITF transport in the upper 100 m of Makassar Strait as well as signatures of the MJO over the Indonesian maritime continent is given in section 3. Section 4 describes an assessment of physical processes pertinent to MJO-forced ITF transport variability during DJFM. Summary and discussion are given in section 5.

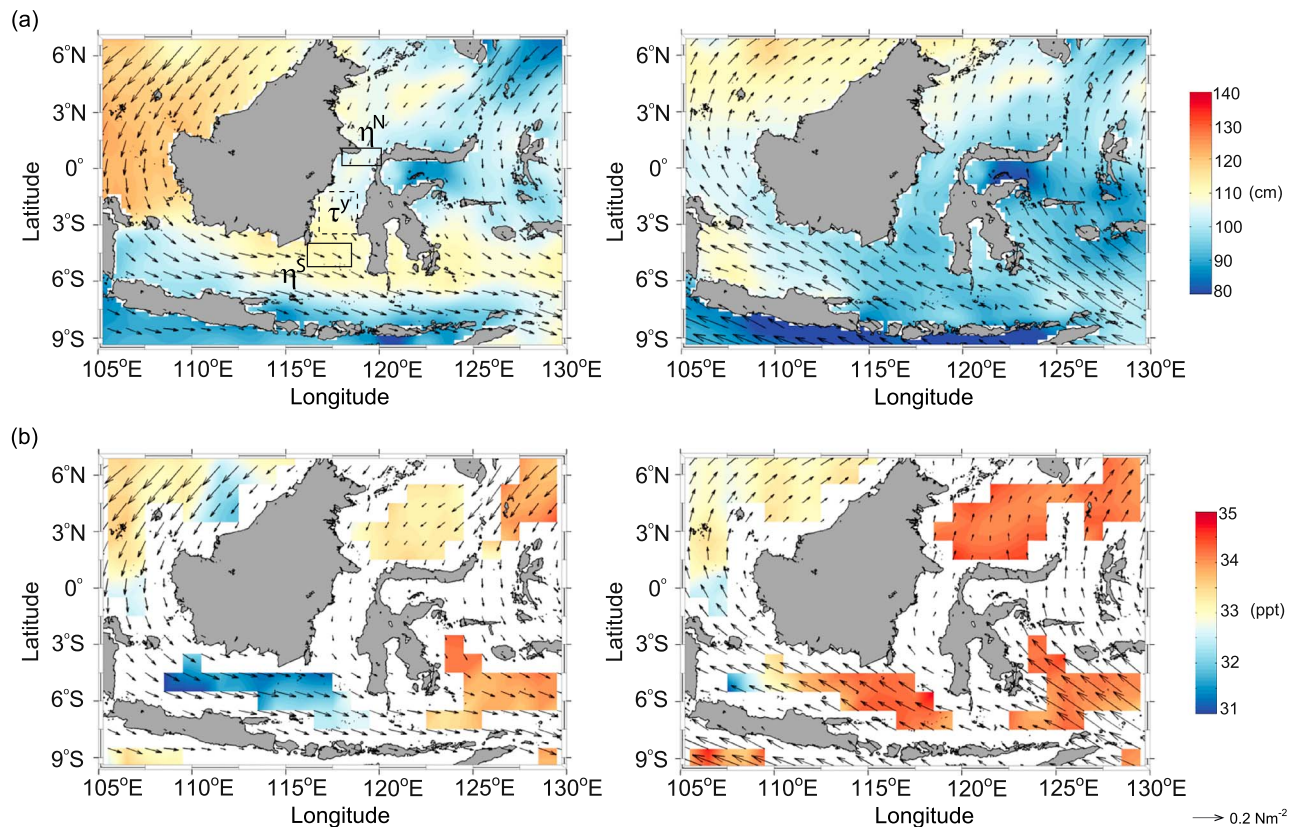


Figure 2. Seasonal averages of (a) sea surface height (η) and (b) sea surface salinity for the months of December–March (left panel) and June–September (right panel) across the central Indonesian maritime continent. Arrows denote wind stress. Solid and dashed rectangles in (a) indicate the areas where η^N , η^S , and τ^y are computed as indicated in the text.

2. Data and Methods

2.1. Moored and Satellite-Retrieved Data

We analyze the ITF time series from a mooring located at the primary inflow pathway of the ITF in Makassar Strait (Figure 1; carries ~77% of the total ITF, Gordon et al., 2010), gathered during two observational programs: The International Nusantara Stratification and Transport (INSTANT) program from January 2004 to December 2006 and the Monitoring of the ITF (MITF) program spanning between January 2007 to August 2011 and August 2013 to August 2017 (Gordon et al., 2008, 2010, 2019). The mooring was deployed at 2°51.9'S, 118°27.3'E and instrumented by a set of acoustic Doppler current profilers and current meters at selected depths, resolving hourly meridional and zonal velocities between 40 and 760 m, while near-surface velocities were excluded due to biases attributed to acoustic reflections off the sea surface. The velocity data were gridded into a 20-m depth interval, low-pass filtered with a cut off frequency of 0.5 cycle per day in order to remove tidal variations and subsequently daily averaged. The gridded and filtered current vectors were subsequently used to compute the along-strait velocity (v) parallel to the along axis of Makassar Strait and across-strait velocity (u). The ITF transport was determined by multiplying the average v profile and the depth-dependent cross-section area of the narrow constriction. The transport sign convention used throughout this paper is that negative values indicate southward transport toward the Indian Ocean. The reader is referred to (Gordon et al., 2008, 2010) for detailed mooring configurations used during the International Nusantara Stratification and Transport and MITF and methods to compute the transport. The moored data can be accessed through <https://www.ldeo.columbia.edu/~bhuber/MITF/>.

The focus of our study is to analyze the ITF variability in the upper 100 m (henceforth referred to surface layer) for the boreal winter periods observed by the Makassar mooring in January 2004 to August 2011 and August 2013 to December 2016. The definition of surface layer used here is consistent with that

given in (Pujiana et al., 2009) that classifies the water column in Makassar Strait into surface layer (surface to 100 m), upper pycnocline (100–150 m), and lower pycnocline (>150 m). The mean base of the surface layer at 100 m is also in agreement with the local Ekman depth (d) at our mooring location.

To provide insights into physical processes relevant with the ITF and MJO over a broader region, remotely sensed data are examined. Daily and gridded satellite-derived sea surface height (η), wind stress (τ), and outgoing longwave radiation (OLR) data, respectively products of Archiving, Validation, and Interpretation of Satellite Oceanographic Data, Institut Français de Recherche pour l'exploitation de la Mer, National Oceanic and Atmospheric Administration Earth Systems Research Laboratory, available between 2004 and 2016 are examined (Bentamy et al., 2002; Ducet et al., 2000; Liebmann & Smith, 1996). Like moored v , along-strait wind stress (τ^y) parallel to the along-strait axis is computed from zonal wind stress (τ^x) and meridional wind stress (τ^y). Along-strait pressure gradient ($\partial\eta$) is estimated by subtracting η averaged in the northern Makassar Strait (η^N) from η averaged in the southern Makassar Strait (η^S). Satellite altimetry-retrieved η data in the Indonesian seas have been validated and reliably used in previous studies (Lee et al., 2017; Passaro et al., 2016; Xu et al., 2016). The η and τ data have a spatial resolution of $0.25^\circ \times 0.25^\circ$, while the OLR data have a spatial resolution of $2.5^\circ \times 2.5^\circ$. The satellite-derived τ and η data are available from <http://marine.copernicus.eu/services-portfolio/access-to-products/>, and the OLR data can be obtained from https://www.esrl.noaa.gov/psd/data/gridded/data.interp_OLR.html.

2.2. MJO Identification

We use the OLR and the real-time multivariate (RMM) index (Wheeler & Hendon, 2004) to define events of the MJO convective (hereafter active) phase in the present analysis. First, the gridded OLR data are averaged at a latitude domain from 5°N to 5°S and then band-pass (20- to 90-day periods) filtered to form a set of intraseasonal OLR data in the longitude-time domain. A MJO event is defined when the OLR contour of -10 W/m^2 is continuously observed between 95°E and 135°E , indicating uninterrupted eastward propagation of MJO convection across the Indonesian seas. Second, the MJO event must be marked by RMM amplitudes exceeding 1 for RMM phases from 4 to 5, implying a complete cycle of the MJO over the Indonesian seas (Figure 3b). Third, zonal wind stress (τ^x) spatially averaged over an area (marked by a box in Figure 1) in the southern Makassar Strait attributed to the MJO active phase event must exceed 0.02 N/m^2 (Figure 3c; Pujiana & McPhaden, 2018; Pujiana et al., 2018). Using the aforementioned criteria, we identify 11 MJO events in Makassar Strait during January 2004 to August 2011 and during August 2013 to December 2016. Neither nonpropagating MJO events nor propagating MJO passages occurring through JJAS are considered in our analysis.

3. Surface Layer ITF Variability

In this section, we will present mean and variations of ITF transport in Makassar Strait, in order to assess contributions of intraseasonal variation in affecting boreal winter reduction of the transport in the surface layer. Mean seasonal cycle of the transport is briefly discussed to provide a sense of the influence of intraseasonal variation in modulating the seasonal cycle. Details on the transport seasonal variability are documented in Gordon et al. (2019).

3.1. Surface Layer Seasonal Variability

The ~ 11 -year measurement of currents in Makassar Strait during January 2004 to August 2011 and August 2013 to December 2016 reveals ITF transport variability across a wide band of timescales (Figures 4a and 4b). Daily averages of total transport of surface layer ITF in Makassar Strait is on average directed toward the Indian Ocean with a mean of $-2.6 \pm 1.1 \text{ Sv}$. Mean seasonal cycle of the total transport clearly exhibits seasonality, with a maximum transport of $-3.2 \pm 0.2 \text{ Sv}$ during JJAS and a minimum transport of $-1.7 \pm 0.6 \text{ Sv}$ during DJFM (blue curve in Figure 4b). Note that the mean seasonal cycle is obtained by smoothing the daily averages of the total transport using a 61-day triangle filter.

The surface layer total transport toward the Indian Ocean was anomalously intensified during JJAS of 2008–2010 in response to prolonged La Niña events (Gordon et al., 2012, 2019), but the transport was anomalously reduced or even reversed during JJAS of 2016 (red curve in Figure 4b). Pujiana et al. (2019) argued that the attenuation of the ITF transport in the surface layer of Makassar Strait observed during boreal summer of 2016 was linked to an extremely strong negative Indian Ocean Dipole event.

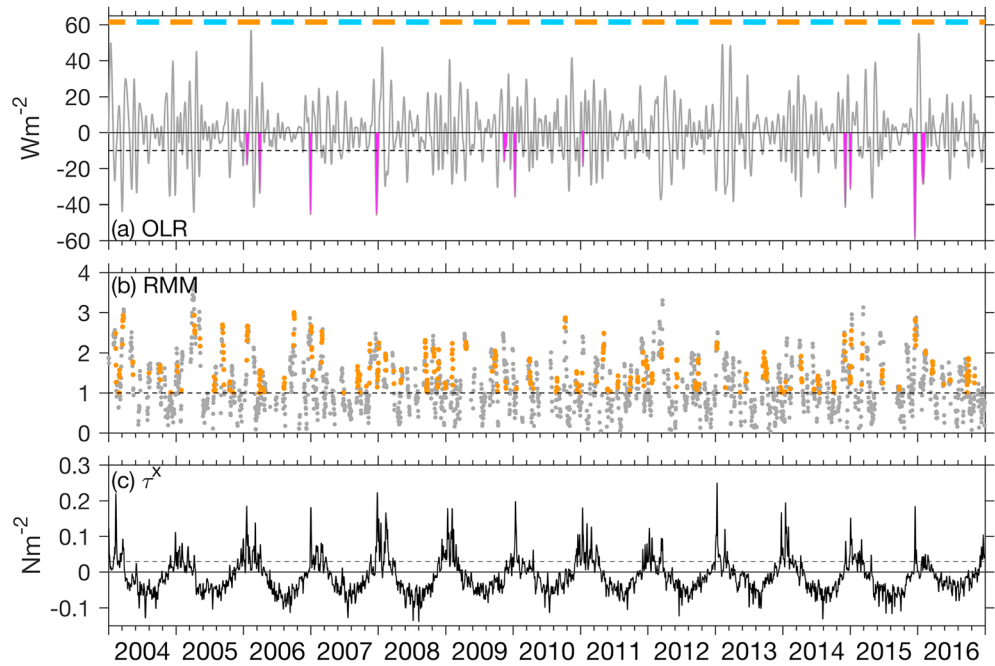


Figure 3. Daily time series of (a) outgoing longwave radiation (OLR), (b) amplitudes of real-time multivariate (RMM) index for phases 3–6, and (c) zonal wind stress (τ^X) observed between January 2004 and December 2016. The OLR and τ^X time series are averages between 3–7°S and 116°E to 118.5°E. The OLR averages are band-pass-filtered (20–90 days) time series, while the τ^X averages are low-pass-filtered (>5 days) time series. Shaded magenta curves mark the active phase of the Madden-Julian Oscillation events as defined in the text. Horizontal dashed line marks an OLR magnitude of -10 W/m^2 . Orange and blue horizontal bars in (a) respectively mark December–March and June–September. Orange dots in (b) demonstrate the RMM amplitudes >1 for phases 4 and 5. Horizontal dashed line in (c) indicates τ^X of 0.02 N/m^2 .

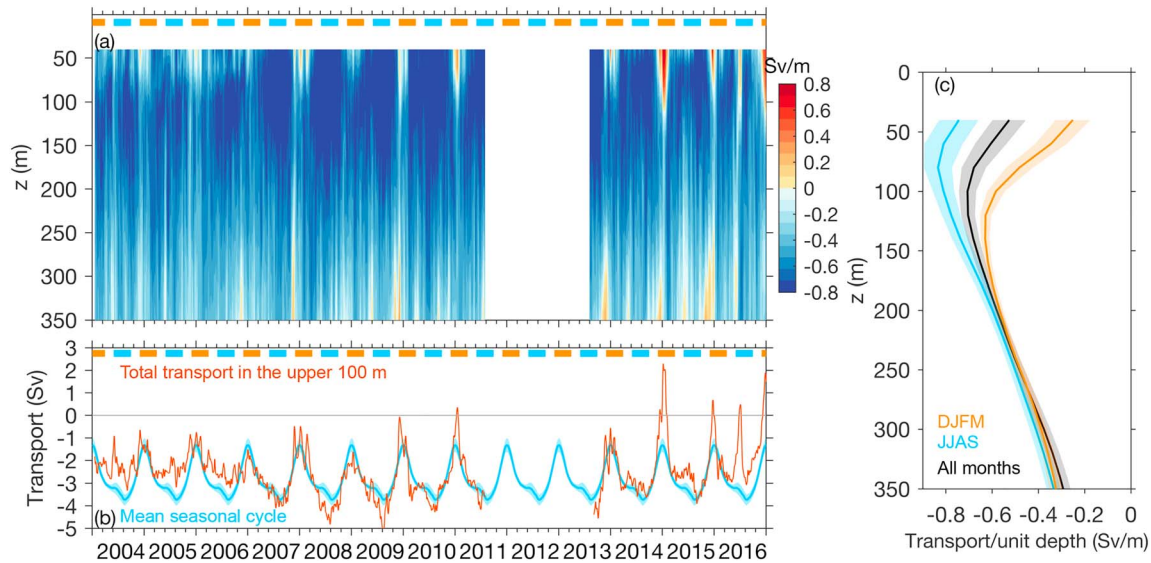


Figure 4. Daily time series of (a) long-strait transport per unit depth in the upper 350 m and (b) total transport in the upper 100 m observed between January 2004 and December 2016 in Makassar Strait. The transport was low-pass filtered (>5 days). Orange and blue horizontal bars in (a) respectively mark December–March (DJFM) and June–September (JJAS). Blue curve in (b) indicates mean seasonal cycle of the respective total transport. The mean seasonal cycle was obtained by smoothing the total transport using a 61-day triangle filter. (c) Profiles of the transport per unit depth shown in (a) averaged for DJFM (orange), JJAS (blue), and all months (black). Negative values of the transport indicate ITF transport toward the Indian Ocean. Color-coded shades indicate 95% bootstrap confidence limits.

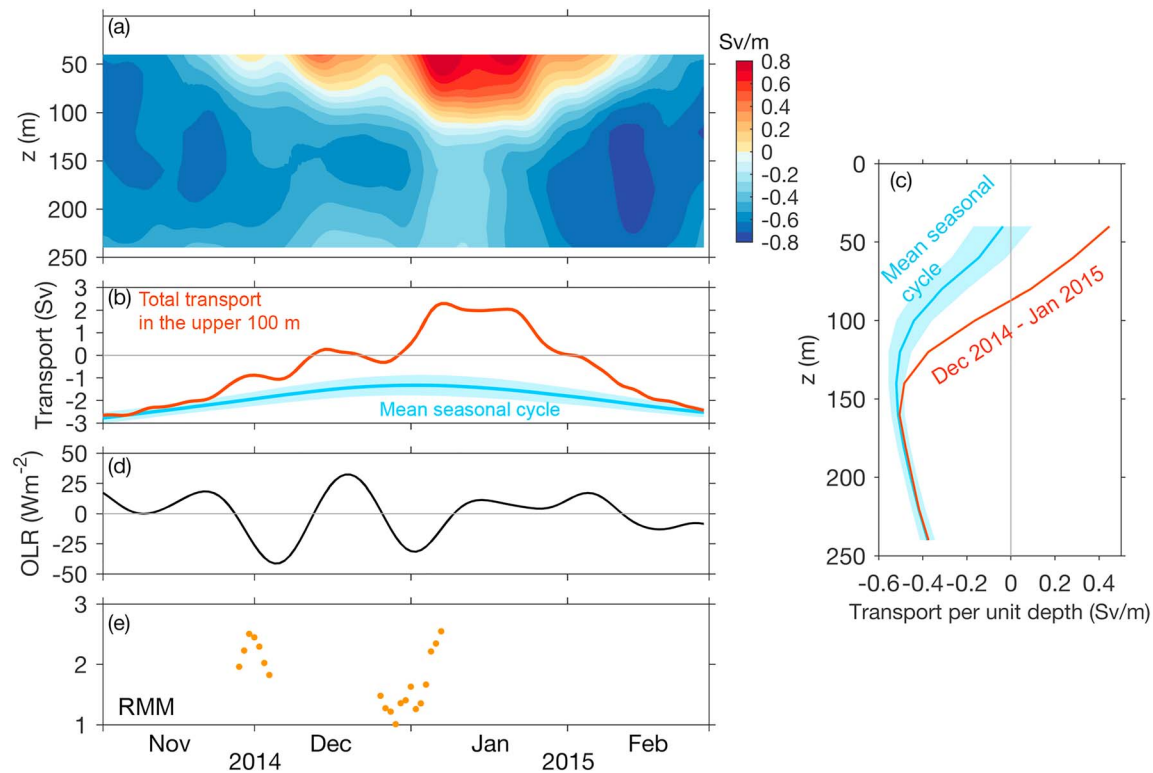


Figure 5. As in Figure 4 but for November 2014 to February 2015. (d) Outgoing longwave radiation (OLR) time series averaged between 3–7°S and 116–119°E. (e) Amplitudes of real-time multivariate (RMM) index for phases 4 and 5. Color-coded shades in (b) and (c) indicate 95% bootstrap confidence limits.

Anomalous events also marked surface layer ITF transport during DJFM. For example, notable events occurred through December 2014 to March 2015, December 2015, and December 2016, during which the surface layer transport was substantially weaker than normal (Figure 4b). Signature of seasonal variability of ITF transport in Makassar Strait is most pronounced in the surface layer (Figure 4c). The ITF transport, averaged over the observation period, is maximum near the base of the surface layer at 100 m, and it weakens with depth (black curve in Figure 4c). The average profiles for DJFM and JJAS indicate that the depth of the maximum transport shifts greater depth as the ITF transitions from an energetic period in JJAS to a weaker phase in DJFM (Gordon et al., 2010, 2019).

3.2. Surface Layer Intraseasonal Variability

As discussed above, the ITF transport in the Makassar Strait surface layer displays a seasonal cycle in which the ITF respectively relaxes and intensifies the most during DJFM and JJAS. Coupled with the seasonal cycle, intraseasonal variation appears to govern the ITF variability during DJFM. For example, monthly variation modulates the seasonal cycle of the ITF to yield the weakest surface layer ITF transport through December 2014 to March 2015 (Figures 5a–5c). Figure 5b shows that the monthly variation contributes to further weaken the surface layer transport by up to 4 Sv relative to its mean seasonal cycle. The monthly surface layer ITF pulses correspond to two strong MJO events characterized by band-pass-filtered OLR < -10 W/m² and RMM > 1 for phases 4 and 5 (Figures 5d and 5e).

To explore the significance of nonseasonal variations to Makassar Strait surface layer variability, the anomalies of the ITF transport (henceforth referred to transport anomalies) are determined by subtracting the mean seasonal cycle from the daily averages of low-pass-filtered (>5 days) surface layer transport. The dominant variations characterizing the transport anomalies vary from 20 to 120 days, particularly during DJFM (Figures 6a and 6b). The boreal winter anomalies during January 2004 to August 2011 were generally attributable to variations with timescales of 30–60 days, while those observed within the August 2013 to December 2016 time frame showed pronounced variations at

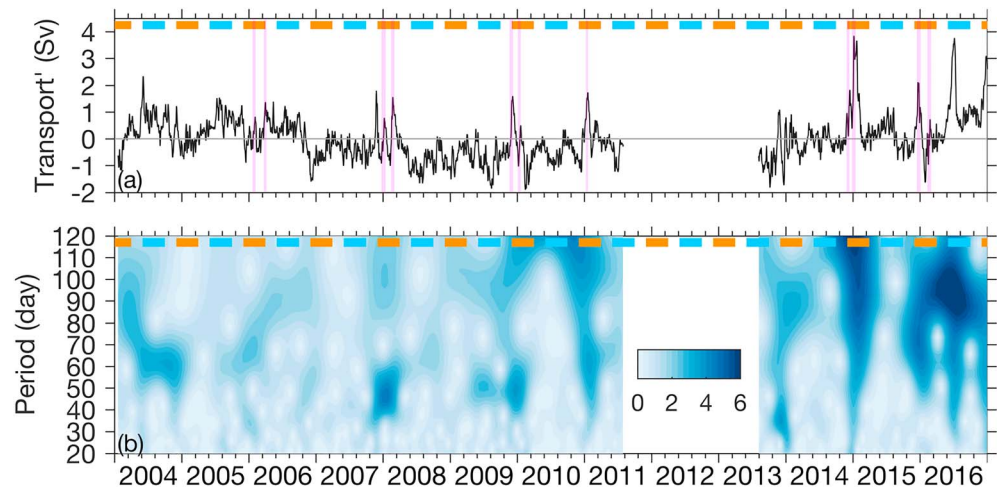


Figure 6. Daily time series of (a) transport anomalies in the surface layer and (b) its wavelet transform observed between January 2004 and December 2016 in Makassar Strait. Positive values of the transport anomalies indicate reduced Indonesian Throughflow transport toward the Indian Ocean. Orange and blue horizontal bars in (a) and (b) respectively mark December–March and June–September. Vertical magenta lines in (a) mark the active phase of the 11 Madden-Julian Oscillation events.

timescales of 60–120 days (Figure 6b). In addition, the boreal winter intraseasonal activity of the surface layer transport was more energetic during 2014–2016 than during earlier record. Physical processes governing the increased intraseasonal variance during boreal winters of 2014–2016 remain unaccounted for, but we speculate that the increased intraseasonal activity, particularly during December 2014 to March 2015 and December 2015 to March 2016, coincided with a period of strong El Niño (Gordon et al., 2019).

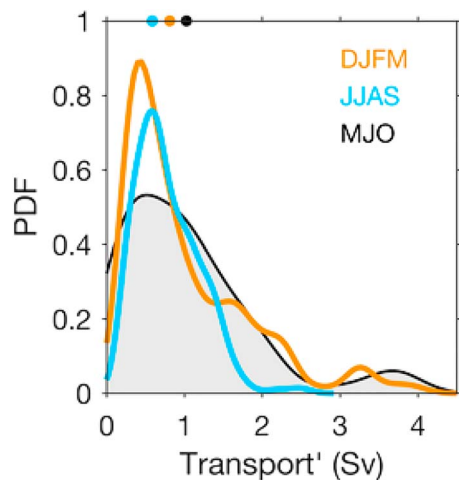


Figure 7. Probability density functions of Indonesian Throughflow transport anomalies greater than 0 Sv in the surface layer of Makassar Strait through December–March (DJFM; orange), June–September (JJAS; blue) and during the MJO events over the course of January 2004 to August 2011 and August 2013 to December 2016. The JJAS distribution excludes the anomalies during boreal summer 2016. Color-coded circles indicate the average values of the anomalies. MJO = Madden-Julian Oscillation; PDF = probability density function.

During boreal summer months, the transport anomalies generally showed a weak signature of intraseasonal variation, except during JJAS 2016 when the anomalies were characterized by variations with a spectral peak ranging from 20 to 120 days and centered at around 90–100 days (Figure 6b). Strong intraseasonal variations governing the transport anomalies of surface layer during JJAS 2016 may relate to intensified intraseasonal activities of η along southern coast of Sumatra and Java prior to and during an extreme negative Indian Ocean Dipole period during boreal summer and fall 2016 (Lim & Hendon, 2017; Lu et al., 2018; Pujiana et al., 2019).

Distributions of transport anomalies indicate that large positive anomalies occur more frequently in DJFM than in JJAS (Figure 7), implying that intraseasonal processes that reduce ITF transport in the surface layer of Makassar Strait are more active in boreal winter than in boreal summer. The average values of positive transport anomalies observed in DJFM and JJAS are 1 and 0.6 Sv, respectively.

Increased intraseasonal activity during DJFM is also evident in the atmosphere over the maritime continent (Zhang & Dong, 2004). Using OLR as a proxy for the MJO, Napitu et al. (2015) demonstrated enhanced (weakened) intraseasonal OLR variation in DJFM (JJAS) over the Indonesian seas. They also argued that MJO air-sea fluxes accounted for substantial variances of the intraseasonal SST. Since the MJO and SST are coupled in the Indonesian seas (Napitu et al., 2015), the former may play a role to force intraseasonal variation of the transport anomalies in the surface layer of Makassar Strait.

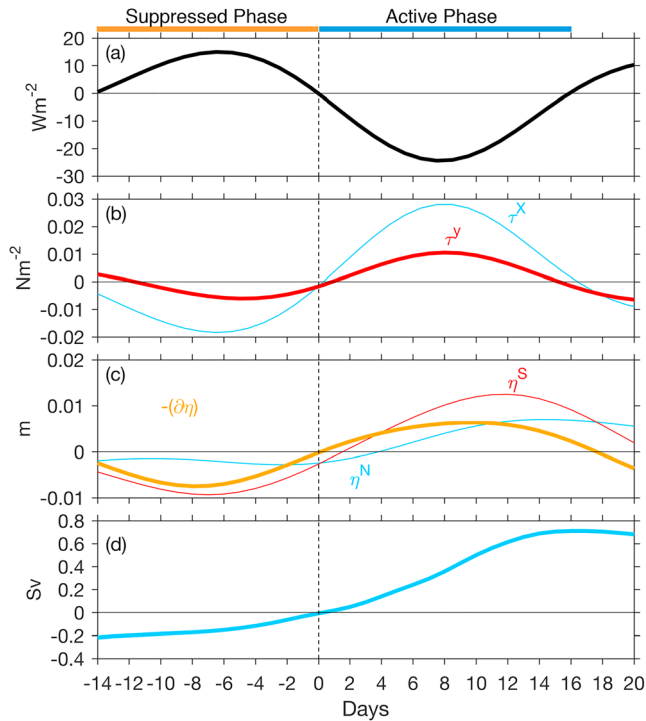


Figure 8. Composites of time series of (a) outgoing longwave radiation, (b) τ^X and along-strait wind stress, τ^Y , and (c) η averaged in the northern (η^N) and southern (η^S) Makassar Strait as indicated in the text, and (d) surface layer transport for the 11 Madden-Julian Oscillation events observed during December–March of 2004 to mid-2011 and September 2013 to December 2016. Positive τ^X (τ^Y) indicates eastward (northward along-strait) wind stress.

in the western part of the basin and decreased η in the southern Makassar Strait (Figure 9a). An increase in southward Ekman transport due to westward wind anomalies might also account for reduced η^S , creating increased southward pressure gradient along the strait (Figure 8c). Both westward τ^X and southward τ^Y weaken as the MJO condition transitions from the suppressed phase to the onset of the active phase (Figures 8b, 9a, and 9b).

As the MJO turns to its active phase, OLR becomes negative and eastward τ^X and northward τ^Y gradually strengthen (Figures 8a and 8b). It takes about ~ 8 days for both OLR and the wind stresses attributed to the MJO events to reach their peak values during the active phase, and the absolute magnitudes of τ^X , τ^Y , and OLR are twice as big at the peak of the active phase as at the peak of the suppressed phase (Figures 8a and 8b). In response to intensified eastward τ^X , an increase in η^S is observed (Figure 8c). An increase in η^S during the active phase is likely forced by eastward wind anomalies-driven northward Ekman transport over Java and Flores Seas that piles up surface water in the southern Makassar Strait (Figures 9c and 9d). η^N also increases during the active MJO phase, particularly along the western coast of Sulawesi but at a slower rate than η^S , resulting in a northward pressure gradient (Figures 8c, 9c, and 9d).

During the active phase, the Makassar Strait surface layer responds to the intensification of northward τ^Y by accelerating parallel to the prevailing along-strait wind stress and hence enhancing positive transport anomalies, resulting in a decrease in the overall surface layer transport (Figures 8d, 9c, and 9d). The increased northward pressure gradient and northward τ^Y , together, set up a favorable condition for positive transport anomalies, resulting in an overall reduction in ITF transport in the surface layer. The maximum positive transport anomaly, about +1 Sv, lags the strongest τ^Y by a few days such that it occurs over a period when the wind stress is substantially reduced and OLR resumes to be positive (Figures 8b and 8d).

OLR time series, averaged between 3–7°S and 116–119°E, and ITF transport anomalies are statistically coherent at timescales between 60–90 days, with the magnitude of squared coherence ranging between 0.6 and 0.7 and the transport anomalies lagging the OLR by 5–8 days (not shown). The coherence between the transport anomalies and OLR time series and its respective lags may imply a causative relationship between the MJO and surface layer ITF.

To further explore the relationship between the MJO and surface layer ITF, MJO signatures attributed to passage of the 11 MJO events traversing from the eastern Indian Ocean to western Pacific Ocean, via the Indonesian seas, observed during boreal winter months of January 2004 to August 2011 and August 2013 to December 2016, are analyzed. To simplify the analysis, we evaluate composite averaged time series of band-pass-filtered (20–90 days) OLR, τ^X , τ^Y , η^N , η^S , $-(\eta^N - \eta^S)$, and transport anomalies of surface layer ITF data attributed to the 11 MJO events. The composite is obtained by averaging the time series for the MJO events from 14 days prior to the active phase onset to 16 days after the onset, resolving the average cycle of a MJO passage over the Indonesian seas. The largest rate of change of OLR marks the onset time (day = 0).

The composites indicate that the suppressed phase of the MJO over the area encompassing Makassar Strait is marked with less cloudy sky (OLR > 0), easterly winds over southern Makassar Strait, northerly winds over the mooring in Makassar Strait, pressure head into the southern Makassar Strait, and negative anomalies of surface layer transport (Figures 8a–8d). A snapshot of the aforementioned atmospheric and oceanic signatures during the suppressed phase (day = –4) over a broader region in the Indonesian seas clearly demonstrates positive OLR values prevailing over most the region, with westward winds extending from Java to Banda Seas, southward winds set in over the Makassar Strait (Figure 9a). Westward wind anomalies over Java Sea lead to increased η

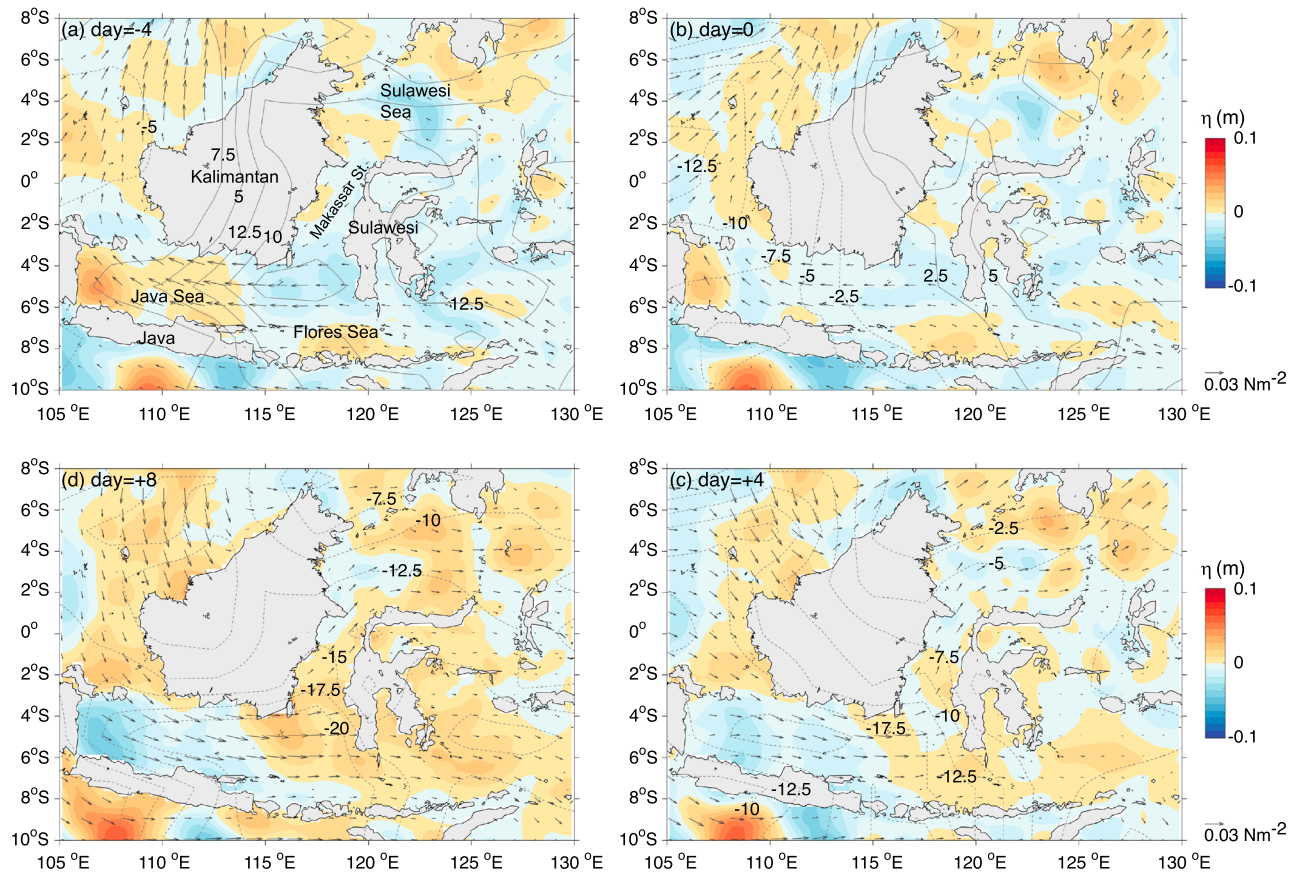


Figure 9. Snapshots of compositing η , outgoing longwave radiation (contours), and wind stress (arrows) for the Madden-Julian Oscillation events observed over the central Indonesian maritime continent over the course of 2004–2016. Dashed (solid) contours denote negative (positive) outgoing longwave radiation.

4. Momentum Transfers

As discussed above, the satellite-derived and moored data demonstrate that 11 boreal winter MJO events affect surface wind stress, along-strait pressure gradient, and surface layer transport anomaly in the Makassar Strait. In this section, we further quantify the contributions of surface forcing and oceanic processes to regulate the dynamic response of the surface layer to the MJO events. The quantification allows us to assess the role of the MJO to regulate reduced ITF transport events in the surface layer of Makassar Strait in DJFM through the observation period, which focuses on the temporal evolution during the active phase of the MJO. To assess the contributions, we analyze the along-strait momentum budget using a simplified equation for horizontal momentum conservation integrated between the surface and a fixed depth of $h = 100$ m. The equation is given as follows:

$$\frac{\partial \bar{v}}{\partial t} = -g \frac{\partial \eta}{\partial y} + \frac{\tau^y}{\rho h} + R, \quad (1)$$

where $\bar{v} = \frac{1}{h} \int_0^h v dz$ is vertically averaged along-strait velocity observed in the surface layer, g is gravity acceleration, ρ is the background density set equal to $1,023 \text{ kg/m}^3$, and R is the residual. A linear extrapolation is employed to estimate v between the shallowest acoustic Doppler current profiler depth bin at 40 m and the surface. The first term on the right-hand side of (1) expresses momentum component due to the along-strait pressure gradient, the second term represents momentum transferred from the along-strait surface wind stress, and the third term contains unresolved physical processes (the turbulent momentum flux at the base of the surface layer, the along-strait divergence of mean v , the upwelling of along-strait momentum, and the mesoscale eddy flux) plus errors associated with the measurements.

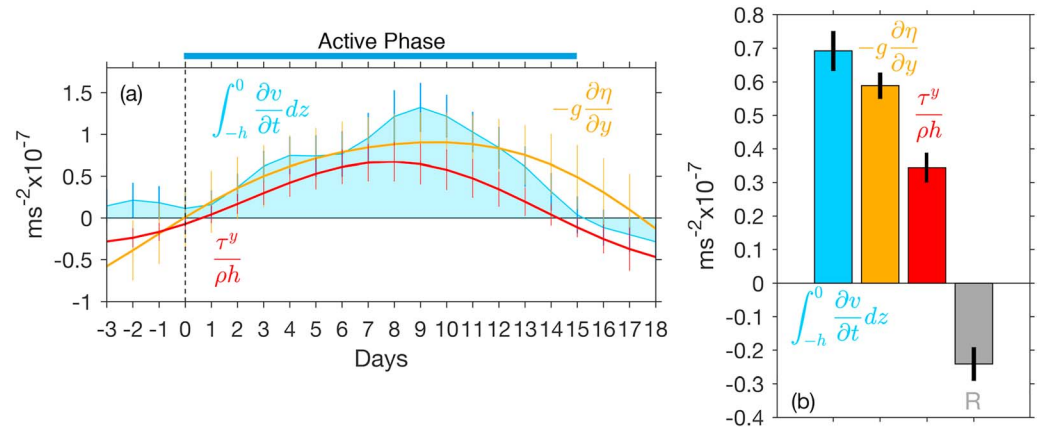


Figure 10. (a) Composites of time series of each term of the momentum equation within the surface layer of Makassar Strait for the Madden-Julian Oscillation events observed during 2004 to August 2011 and August 2013 to 2016. Shaded blue area indicates along-strait acceleration, red curve indicates Reynolds stress at the surface, and yellow curve shows momentum input from along-strait pressure gradient force. Color-coded vertical lines show 95% bootstrap confidence limits. (b) The mean magnitude of each term in (a) during the active phase from day = 0 to day = 15. Gray bar accounts for the residual. Positive (negative) values indicate northward (southward) along-strait acceleration.

A band-pass filter (20–90 days) is employed to isolate intraseasonal variations of time series of each term of (1). A composite of temporal evolution of the momentum budget terms encompassing the active phase of the MJO events is determined using the filtered time series. Based on the composite time series, averages of all terms of (1) for the MJO events during the active phase from day = 0 to day = 15 are subsequently computed. Note that the vertical integration of the term on left hand side of (1) is approximated using a trapezoidal rule.

Momentum balance for the MJO case illustrates that the surface layer is accelerated northward during the active phase of the MJO events (positive acceleration, shaded blue curve in Figure 10a). Northward along-strait wind stress and northward pressure gradient transfer northward momentum into the surface layer (Figure 10a). The τ^y and $\partial \eta / \partial y$ result in northward acceleration, each averaging 0.58×10^{-7} and $0.34 \times 10^{-7} \text{ m/s}^2$, respectively (Figure 10b). The combined momentum transfer from the wind stress and pressure gradient, however, exceeds the average magnitude of the observed acceleration by 34% (Figure 10b) so that the residual should act to decelerate the northward acceleration of the surface layer.

The residual might be attributable to turbulent momentum flux at the base of the surface layer as turbulence would diffuse the northward momentum downward and hence decelerate the northward acceleration in the layer. Pujiana et al. (2018) suggested that the vertical divergence of Reynold stresses was fundamental in governing the surface layer acceleration in response to the MJO in the equatorial Indian Ocean. They posited that turbulent Reynold stress at the base of the surface layer was about 65% of surface wind stress. Assume the relationship between surface wind stress and turbulent stress at the base of the surface layer holds in Makassar Strait, the average magnitude of southward acceleration due to turbulent momentum flux at the base of the surface layer would be $0.22 \times 10^{-7} \text{ m/s}^2$, within the order of the average magnitude of excess northward acceleration due to combined τ^y and $\partial \eta / \partial y$ over the average magnitude of acceleration observed in the surface layer.

5. Summary and Discussion

We have identified and analyzed physical processes regulating the ITF variability in the surface layer, particularly those varying at intraseasonal timescales, inferred from observations in Makassar Strait between January 2004 to August 2011 and August 2013 to December 2016. The observations confirm the presence of austral monsoon-driven seasonal cycle of the surface layer southward throughflow, with minimum (maximum) transport occurring during DJFM (JJAS). Reduced ITF transport in the surface layer during DJFM is not only attributable to the monsoon but also forced by intraseasonal events. Transport anomalies of the surface layer markedly demonstrate 1- to 3-month variations during DJFM. We propose that the MJO, coupled

with the monsoon, contributes to regulate ITF transport variation in the Makassar Strait surface layer during boreal winter.

Over the course of the observation, 11 MJO events making a complete eastward propagation over the Indonesian seas from the eastern Indian Ocean to the western Pacific Ocean are identified, and their signatures within the Makassar Strait throughflow are analyzed. Impacts of the suppressed and active phases of the 11 MJO events on surface forcing and oceanic processes governing the surface layer ITF during boreal winter can be summarized as follows:

1. During the suppressed phase of the MJO events, westward and southward wind anomalies respectively prevail over Java Sea and Makassar Strait. The westward wind-driven Ekman transport likely lowers sea surface in the southern Makassar Strait, resulting in an increase in southward along-strait pressure gradient. Negative transport anomalies that reflect increased southward ITF transport in the surface layer mark the suppressed phase.
2. During the active phase of the MJO events, the prevailing wind anomalies over Java Sea turn eastward and northward wind anomalies prevail over the Makassar Strait. Supported by the eastward wind-driven Ekman transport, surface water accumulation is observed in the southern Makassar Strait, yielding northward pressure gradient along the strait. The MJO events force positive transport anomalies (or northward transport), which may cause a substantial reduction of the southward transport of surface layer ITF up to 4 Sv. On average, the MJO-forced northward transport is about +0.45 Sv, which is about a quarter of the average southward transport of the boreal winter surface layer ITF amounting to 1.7 Sv.
3. Analysis of the momentum budget in the surface layer indicates that the excess of northward momentum due to combined pressure gradient and surface Reynold stress over southward momentum attributed to the residual terms accounts for northward acceleration in the surface layer during the active phase of the MJO events.

While most previous studies have documented that the MJO has indirect influence on ITF variability at depths beneath the surface layer through Kelvin waves (Drushka et al., 2010; Schiller et al., 2010; Zhou & Murtugudde, 2010), our results provide a new insight into the direct impact of the MJO on the surface layer ITF. Using a numerical experiment, Shinoda et al. (2016) investigated the response of the ITF to the MJO between fall 2010 and spring 2011. They, in principle, suggested that the surface layer in Makassar Strait responded to a MJO forcing by generating northward current. Although a quantitative assessment on factors controlling the northward current was not presented in their analyses, they argued that the northward current in Makassar Strait was associated with MJO-forced coastal Kelvin waves originating from the Indian Ocean. Our results, however, attribute the northward current as a response of the surface layer to changes in along-strait pressure gradient and wind induced by more localized influence of the MJO. The northward current in the surface layer during the MJO does not show Indian Ocean Kelvin wave characteristics, such as upward phase propagation, which are documented in Pujiana et al. (2013).

In the equatorial Indian Ocean, the upper ocean responds to a passage of the MJO through the formation of a strong eastward current, and the dynamic of the eastward jet is mainly controlled by wind stress, subsurface turbulence, and advection of momentum (Moum et al., 2016; Pujiana et al., 2018; Pujiana & McPhaden, 2018). As in the equator, the role of Coriolis to regulate motions in the surface layer appears to be negligible in Makassar Strait as well. Thus, nonlinear terms such as turbulent momentum flux and along-strait advection of momentum likely forms the residual component of the surface layer response to the MJO in Makassar Strait. A more extensive approach, involving a coupled ocean-atmosphere general circulation model, is required to quantitatively examine how each term of the equation of motion regulates the surface layer response to the MJO in Makassar Strait.

In addition to reducing the southward throughflow within Makassar Strait, the MJO-driven current also substantially alters the meridional SST gradient. Shinoda et al. (2016) indicated that a meridional SST gradient is set up along the Makassar Strait following the MJO cycle, where the southern Makassar Strait was observed colder than to the north. Colder SST in the southern Makassar Strait and Flores Sea might, however, be a product of more intense MJO air-sea interaction in that particular area than over the northern Makassar Strait. Napitu et al. (2015) showed that upward net surface heat flux attributed to the MJO wind during boreal winter cools the SST in the Indonesian seas, particularly those located in the Southern Hemisphere. It is also possible that subsurface turbulent mixing, triggered by increased instability due to

northward flow near the surface overlying southward flow at deeper depth, might promote downward heat transfer leading to colder SST in Makassar Strait. Quantifying competing processes, from advection to sub-surface turbulent mixing to air-sea heat flux, which regulates SST along the ITF pathways or the Indonesian Seas in general during the MJO, is an open question.

Acknowledgments

We are grateful for continuing support from the Ministry of Marine Affairs and Fisheries of the Republic of Indonesia, particularly the Institute for Marine Research and Observation, to maintain and service the Makassar Strait mooring. A. M. N. acknowledges the Schlumberger Foundation for the Faculty for the Future award, and K. P. performed this research under a National Research Council award at the National Oceanic and Atmospheric Administration (NOAA) PMEL. Helpful comments from two anonymous reviewers and the assigned editor on an earlier version of the manuscript are appreciated. This research was funded by NOAA, Division of Climate Observations, U.S. Department of Commerce via grant UCAR Z15-17551. The statements, findings, conclusions, and recommendations are those of the authors and do not necessarily reflect the views of NOAA or the Department of Commerce. The moored data can be accessed through <https://www.ideo.columbia.edu/~bhuber/MITF/>, the satellite-derived wind stress and sea surface height data are available from <http://marine.copernicus.eu/services-portfolio/access-to-products/>, and the OLR data can be obtained from https://www.esrl.noaa.gov/psd/data/gridded/data.interp_OLR.html. Lamont-Doherty Earth-Observatory contribution number 8307. PMEL contribution number 4971.

References

- Bentamy, A., Katsaros, K., Drennan, W., & Forde, E. (2002). Daily surface wind fields produced by merged satellite data. *Gas Transfer at Water Surfaces*, 127, 343–349.
- Chen, X., Qiu, B., Chen, S., Cheng, X., & Qi, Y. (2018). Interannual modulations of the 50-day oscillations in the Celebes Sea: Dynamics and impact. *Journal of Geophysical Research: Oceans*, 123, 4666–4679. <https://doi.org/10.1029/2018JC013960>
- Drushka, K., Sprintall, J., Gille, S. T., & Brodjonegoro, I. (2010). Vertical structure of Kelvin waves in the Indonesian Throughflow exit passages. *Journal of Physical Oceanography*, 40(9), 1965–1987. <https://doi.org/10.1175/2010JPO4380.1>
- Ducet, N., Le Traon, P.-Y., & Reverdin, G. (2000). Global high-resolution mapping of ocean circulation from TOPEX/Poseidon and ERS-1 and-2. *Journal of Geophysical Research*, 105(C8), 19,477–19,498. <https://doi.org/10.1029/2000JC900063>
- Gordon, A. L. (1986). Inter-ocean exchange of thermocline water. *Journal of Geophysical Research*, 91(C4), 5037–5046. <https://doi.org/10.1029/JC091iC04p05037>
- Gordon, A. L., Huber, B. A., Metzger, E. J., Susanto, R. D., Hurlburt, H. E., & Adi, T. R. (2012). South China Sea throughflow impact on the Indonesian throughflow. *Geophysical Research Letters*, 39, L11602. <https://doi.org/10.1029/2012GL052021>
- Gordon, A. L., Napitu, A., Huber, B. A., Gruenborg, L. K., Pujiana, K., Agustiani, T., et al. (2019). Makassar Strait Throughflow seasonal and interannual variability, an overview. *Journal of Geophysical Research: Oceans*, 124. <https://doi.org/10.1029/2018JC014502>
- Gordon, A. L., Sprintall, J., van Aken, H. M., Susanto, D., Wijffels, S., Molcard, R., et al. (2010). The Indonesian throughflow during 2004–2006 as observed by the INSTANT program. *Dynamics of Atmospheres and Oceans*, 50(2), 115–128. <https://doi.org/10.1016/j.dynatmoce.2009.12.002>
- Gordon, A. L., Susanto, R. D., Ffield, A., Huber, B. A., Pranowo, W., & Wirasantosa, S. (2008). Makassar Strait throughflow, 2004 to 2006. *Geophysical Research Letters*, 35, L24605. <https://doi.org/10.1029/2008GL036372>
- Lee, T., Farrar, J. T., Arnault, S., Meyssignac, B., Han, W., & Durland, T. (2017). Monitoring and interpreting the tropical oceans by satellite altimetry. In *Satellite Altimetry Over Oceans and Land Surfaces* (pp. 231–270). Boca Raton, FL: CRC Press.
- Liebmann, B., & Smith, C. A. (1996). Description of a complete (interpolated) outgoing longwave radiation dataset. *Bulletin of The American Meteorological Society*, 77, 1275–1277.
- Lim, E.-P., & Hendon, H. H. (2017). Causes and predictability of the negative Indian Ocean Dipole and its impact on La Niña during 2016. *Scientific Reports*, 7(1), 12619. <https://doi.org/10.1038/s41598-017-12674-z>
- Lu, B., Ren, H. L., Scaife, A. A., Wu, J., Dunstone, N., Smith, D., et al. (2018). An extreme negative Indian Ocean Dipole event in 2016: Dynamics and predictability. *Climate Dynamics*, 51(1–2), 89–100. <https://doi.org/10.1007/s00382-017-3908-2>
- Moum, J. N., Pujiana, K., Lien, R. C., & Smyth, W. D. (2016). Ocean feedback to pulses of the Madden-Julian Oscillation in the equatorial Indian Ocean. *Nature Communications*, 7(1). <https://doi.org/10.1038/ncomms13203>
- Napitu, A. M., Gordon, A. L., & Pujiana, K. (2015). Intraseasonal sea surface temperature variability across the Indonesian Seas. *Journal of Climate*, 28(22), 8710–8727. <https://doi.org/10.1175/JCLI-D-14-00758.1>
- Passaro, M., Dinardo, S., Quartly, G. D., Snaith, H. M., Benveniste, J., Cipollini, P., & Lucas, B. (2016). Cross-calibrating ALES Envisat and CryoSat-2 Delay-Doppler: A coastal altimetry study in the Indonesian Seas. *Advances in Space Research*, 58(3), 289–303. <https://doi.org/10.1016/j.asr.2016.04.011>
- Potemra, J. T., & Lukas, R. (1999). Seasonal to interannual modes of sea level variability in the western Pacific and eastern Indian Oceans. *Geophysical Research Letters*, 26(3), 365–368. <https://doi.org/10.1029/1998GL900280>
- Pujiana, K., Gordon, A. L., Metzger, E. J., & Ffield, A. L. (2012). The Makassar Strait pycnocline variability at 20–40 days. *Dynamics of Atmospheres and Oceans*, 53–54, 17–35. <https://doi.org/10.1016/j.dynatmoce.2012.01.001>
- Pujiana, K., Gordon, A. L., & Sprintall, J. (2013). Intraseasonal Kelvin wave in Makassar Strait. *Journal of Geophysical Research: Oceans*, 118, 2023–2034. <https://doi.org/10.1002/jgrc.20069>
- Pujiana, K., Gordon, A. L., Sprintall, J., & Susanto, R. D. (2009). Intraseasonal variability in the Makassar Strait thermocline. *Journal of Marine Research*, 67(6), 757–777. <https://doi.org/10.1357/002224009792006115>
- Pujiana, K., & McPhaden, M. J. (2018). Ocean surface layer response to convectively coupled Kelvin waves in the eastern equatorial Indian Ocean. *Journal of Geophysical Research: Oceans*, 123, 5727–5741. <https://doi.org/10.1029/2018JC013858>
- Pujiana, K., McPhaden, M. J., Gordon, A. L., & Napitu, A. M. (2019). Unprecedented response of Indonesian throughflow to anomalous Indo-Pacific climatic forcing in 2016. *Journal of Geophysical Research: Oceans*, 124. <https://doi.org/10.1029/2018JC014574>
- Pujiana, K., Moum, J. N., & Smyth, W. D. (2018). The role of turbulence in redistributing upper-ocean heat, freshwater, and momentum in response to the MJO in the equatorial Indian Ocean. *Journal of Physical Oceanography*, 48(1), 197–220. <https://doi.org/10.1175/JPO-D-17-0146.1>
- Schiller, A., Wijffels, S., Sprintall, J., Molcard, R., & Oke, P. R. (2010). Pathways of intraseasonal variability in the Indonesian Throughflow region. *Dynamics of Atmospheres and Oceans*, 50(2), 174–200. <https://doi.org/10.1016/j.dynatmoce.2010.02.003>
- Shinoda, T., Han, W., Jensen, T. G., Zamudio, L., Joseph Metzger, E., & Lien, R.-C. (2016). Impact of the Madden-Julian Oscillation on the Indonesian Throughflow in the Makassar Strait during the CINDY/DYNAMO Field Campaign. *Journal of Climate*, 29(17), 6085–6108. <https://doi.org/10.1175/JCLI-D-15-0711.1>
- Sprintall, J., Gordon, A. L., Koch-Larrouy, A., Lee, T., Potemra, J. T., Pujiana, K., & Wijffels, S. E. (2014). The Indonesian seas and their role in the coupled ocean-climate system. *Nature Geoscience*, 7(7), 487–492. <https://doi.org/10.1038/ngeo2188>
- Sprintall, J., & Revelard, A. (2014). The Indonesian Throughflow response to Indo-Pacific climate variability. *Journal of Geophysical Research: Oceans*, 119, 1161–1175. <https://doi.org/10.1002/2013JC009533>
- Tozuka, T., Qu, T., & Yamagata, T. (2007). Dramatic impact of the South China Sea on the Indonesian Throughflow. *Geophysical Research Letters*, 34, L12612. <https://doi.org/10.1029/2007GL030420>
- Tozuka, T., Qu, T. D., Masumoto, Y., & Yamagata, T. (2009). Impacts of the South China Sea Throughflow on seasonal and interannual variations of the Indonesian Throughflow. *Dynamics of Atmospheres and Oceans*, 47(1–3), 73–85. <https://doi.org/10.1016/j.dynatmoce.2008.09.001>

- Wheeler, M. C., & Hendon, H. H. (2004). An all-season real-time multivariate MJO index: Development of an index for monitoring and prediction. *Monthly Weather Review*, *132*(8), 1917–1932. [https://doi.org/10.1175/1520-0493\(2004\)132<1917:AARMMI>2.0.CO;2](https://doi.org/10.1175/1520-0493(2004)132<1917:AARMMI>2.0.CO;2)
- Xu, T.-F., Wei, Z.-X., Cao, G.-J., & Li, S.-J. (2016). Pathways of intraseasonal Kelvin waves in the Indonesian Throughflow regions derived from satellite altimeter observation. *Atmospheric and Oceanic Science Letters*, *9*(5), 375–380. <https://doi.org/10.1080/16742834.2016.1208047>
- Yoneyama, K., Zhang, C., & Long, C. N. (2013). Tracking pulses of the Madden–Julian Oscillation. *Bulletin of The American Meteorological Society*, *94*(12), 1871–1891. <https://doi.org/10.1175/BAMS-D-12-00157.1>
- Zhang, C., & Dong, M. (2004). Seasonality in the Madden–Julian Oscillation. *Journal of Climate*, *17*(16), 3169–3180. [https://doi.org/10.1175/1520-0442\(2004\)017<3169:SITMO>2.0.CO;2](https://doi.org/10.1175/1520-0442(2004)017<3169:SITMO>2.0.CO;2)
- Zhang, C. D. (2013). Madden-Julian Oscillation bridging weather and climate. *Bulletin of The American Meteorological Society*, *94*(12), 1849–1870. <https://doi.org/10.1175/BAMS-D-12-00026.1>
- Zhou, L., & Murtugudde, R. (2010). Influences of Madden–Julian oscillations on the eastern Indian Ocean and the maritime continent. *Dynamics of Atmospheres and Oceans*, *50*(2), 257–274. <https://doi.org/10.1016/j.dynatmoce.2009.12.003>